Influences on the global structure of cortical maps

GEOFFREY J. GOODHILL†, KEVIN R. BATES AND P. READ MONTAGUE

Division of Neuroscience, Center for Theoretical Neuroscience, Baylor College of Medicine, Houston, TX 77030, USA (geoff@salk.edu)

SUMMARY

Cortical maps often contain global spatial structure; however, theoretical accounts for their development have generally concentrated on reproducing only local structure. We show that the elastic net model of cortical map formation can closely approximate the global structure of the ocular dominance column map observed in macaque primary visual cortex. A key component is the assumption of spatially non-uniform and anisotropic correlations in the retina. This work shows how genetic and epigenetic effects could combine to establish characteristic global structure in cortical maps.

1. INTRODUCTION

A very common representation of sensory or more abstract information in the cortex is in the form of maps. In these structures, the stimuli to which neurons best respond are similar moving perpendicular to the surface of the cortex, while a smooth progression of optimal stimuli is found moving parallel to the cortex. Many examples can be found in the visual, auditory and somatosensory systems. Each of these maps has a detailed local structure and particular types of pattern occur over the scale of a few columns. However, these maps also contain more global forms of organization. One particularly well-studied example is that of ocular dominance columns in the primate primary visual cortex (V1) (Hubel & Wiesel 1977) (figure 1). Locally, these appear as parallel bands. However, on a global scale these bands show an overall orientation that varies with position in V1, are less parallel to each other in the foveal region, tend to be orthogonal to the borders of the neighbouring visual cortical area and decrease in width from the foveal to more peripheral representations (LeVay *et al.* 1985; Horton & Hocking 1996). It is known experimentally that local map structure (such as the precise position of ocular dominance column borders) is dependent on neural activity; however, the source of global structure is unknown.

Theories for how neural activity influences map formation have been very successful in accounting for local map structure. For instance in the visual cortex, such theories have addressed the formation of ocular dominance columns, orientation maps and disparity tuning (e.g. von der Malsburg 1973; von der Malsburg & Willshaw 1976; Obermayer *et al.* 1990, 1992; Berns *et al.* 1993; for recent reviews see Erwin *et al.* (1995) and Swindale (1996)). Theories addressing the origin of global structure are less common. Regarding topographic distortions, Wolf *et al.* (1994) have argued that the influences of input and target shape, combined with a spatially non-uniform probability that points in the input space are stimulated, could be the source of the discontinuities in overall map topography seen experimentally in some areas of the visual system (see also Wolf *et al.* 1996). Regarding ocular dominance, Swindale (1980) showed that asymmetric growth of the target region could yield globally oriented columns. As discussed by for instance Obermayer *et al.* (1990), anisotropic intracortical connectivity could also cause anisotropic columns. Another suggestion, put forward informally by Levay *et al.* (1985) and later investigated computationally by Jones *et al.* (1991), Goodhill & Willshaw (1994) and Bauer (1995), is that the mapping from the two roughly circular lateral geniculate nucleus (LGN) layers to the roughly elliptical cortex has much less topographic stretching when the two circles are sliced into stripes parallel to the short (dorsal–ventral) axis of the ellipse compared to stripes parallel to the long (medial–lateral) axis. In figure 1 it can be seen that columns indeed run in the dorsal–ventral direction near the representation of the optic disc and more peripherally. However, this theory fails to address the more disordered columnar pattern in the region of the cortex representing the fovea, the bias of the columns to run parallel to the medial–lateral axis in the central region of the operculum and the change in column width between fovea and periphery.

In this paper, we explore the hypothesis that these types of detail in the global structure of ocular dominance columns could arise from *spatially non-uniform* and *anisotropic* correlational structure of activity in the retina. We suggest that the non-uniformity arises due to the increase in retinal ganglion cell (RGC) density proceeding from peripheral to central retina, while the anisotropy could arise due to the asymmetric way in which the retina develops.

† Present address: Georgetown Institute for Cognitive and Computational Sciences, Research Building, Georgetown University Medical Center, 3970 Reservoir Road, Washington, DC, 20007, USA.

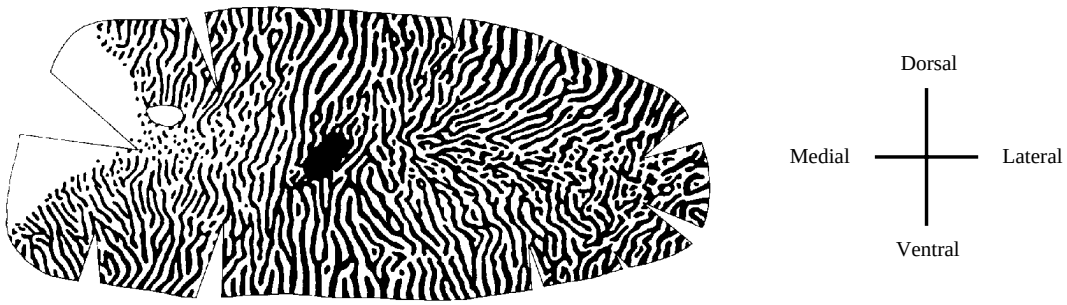

Figure 1. A computer reconstruction of the complete pattern of ocular dominance columns in layer 4 of primary visual cortex of the macaque monkey (right hemisphere). Columns from one eye were labelled by intraocular injection of [^{3}H]proline. The black region is the representation of the optic disc and lateral to this is the operculum. The lateral end represents the fovea and the medial end the periphery. The white far-medial region is the monocular crescent. Between the monocular crescent and the optic disc representation is the calcarine fissure. Reproduced from LeVay *et al.* (1985).

Using the elastic net model for cortical map formation (Durbin & Willshaw 1987; Durbin & Mitchison 1990; Goodhill & Willshaw 1990) we show that a good approximation to the entire experimentally observed pattern of ocular dominance columns can be obtained by manipulating just a small number of parameters. This work demonstrates how influences on target shape, which we suggest could include trophic signals that define the shape of target regions competent for innervation, could combine with activity-dependent effects to govern global features of cortical map organization.

2. THE MODEL

The elastic net model for cortical mapping (Durbin & Willshaw 1987) has previously been shown to reproduce the local structure of ocular dominance (Goodhill & Willshaw 1990) and orientation (Durbin & Mitchison 1990) maps. The algorithm works by trading off two principal constraints: (1) a matching constraint that assays the degree of match (correlated activity) between an afferent axon and a target cortical neuron or site; and (2) a smoothness (regularizing) constraint in the target cortex that encourages axons carrying similar information to innervate neighbouring regions of cortex. Representing the problem at this level of abstraction addresses the role of several competing influences at once, and is often more tractable than approaches that assume particular learning rules operating at synapses.

The two-eye source space is represented by two two-dimensional hexagonal arrays of points aligned parallel to each other in a three-dimensional space (a simplified picture is shown in figure 5). Each fixed point corresponds to a retinal ganglion cell and distances between points represent correlations between locations: correlation strength decreases with increasing distance (Yuille *et al.* 1991, 1996). The cortical units are represented as points in an elastic sheet. Cortical points are connected to their neighbours by elastic bands that enforce the preservation of neighbourhood relationships. The mapping of retinal information onto cortex is represented by the movement of this elastic net between the two arrays of retinal points. Each point in the elastic sheet moves in response to two sets of influences: one pulling it to locations in the source arrays (matching constraint); and an elastic influence pulling it towards its neighbours (smoothing constraint). As development proceeds, the balance of these two influences is gradually changed until the matching term dominates and a stable map results. This representation reduces the correlational structure of the inputs to two basic parameters: the within-eye spacing d and the between-eye spacing l (see figure 5).

Formally, the attractive pull from the retinal layer, representing a weighted matching term for retinal and cortical points, is given by the first term in equation (1). It can also be envisioned as representing competition of the LGN axons for cortical space. The retractive pull induced by stretching the elastic bands, which encourages the algorithm to find smooth solutions, is given by the second term in equation (1). These two types of influences induce a change in the position of cortical points in the elastic sheet according to:

$$\Delta \boldsymbol{y}_j = \alpha \sum_i w_{ij}(\boldsymbol{x}_i - \boldsymbol{y}_j) + \beta k \sum_{n \epsilon N(j)} (\boldsymbol{y}_n - \boldsymbol{y}_j), \quad (1)$$

where $\Delta \boldsymbol{y}_j$ is the change in the position of the cortical point j, $N(j)$ indexes the neighbours of $\boldsymbol{y}_j$, $\boldsymbol{x}_i$ is the fixed position of LGN point i, α and β are constants that scale the relative influence of the two influences and k is another scaling parameter (see later). The first term describes a pull in direction $(\boldsymbol{x}_i - \boldsymbol{y}_j)$ of magnitude w_{ij} from LGN point i to cortical point j. w_{ij} is defined as

$$w_{ij} = \frac{\Phi(|\boldsymbol{x}_i - \boldsymbol{y}_j|, k)}{\sum_p \Phi(|\boldsymbol{x}_i - \boldsymbol{y}_p|, k)}, \quad (2)$$

where p indexes cortical points, and Φ is given by

$$\Phi(|\boldsymbol{x}_i - \boldsymbol{y}_j|, k) = \exp\left(\frac{-|\boldsymbol{x}_i - \boldsymbol{y}_j|^2}{2k^2}\right). \quad (3)$$

w_{ij} represents the normalized pull of LGN point i on cortical point j. k sets the effective range of the

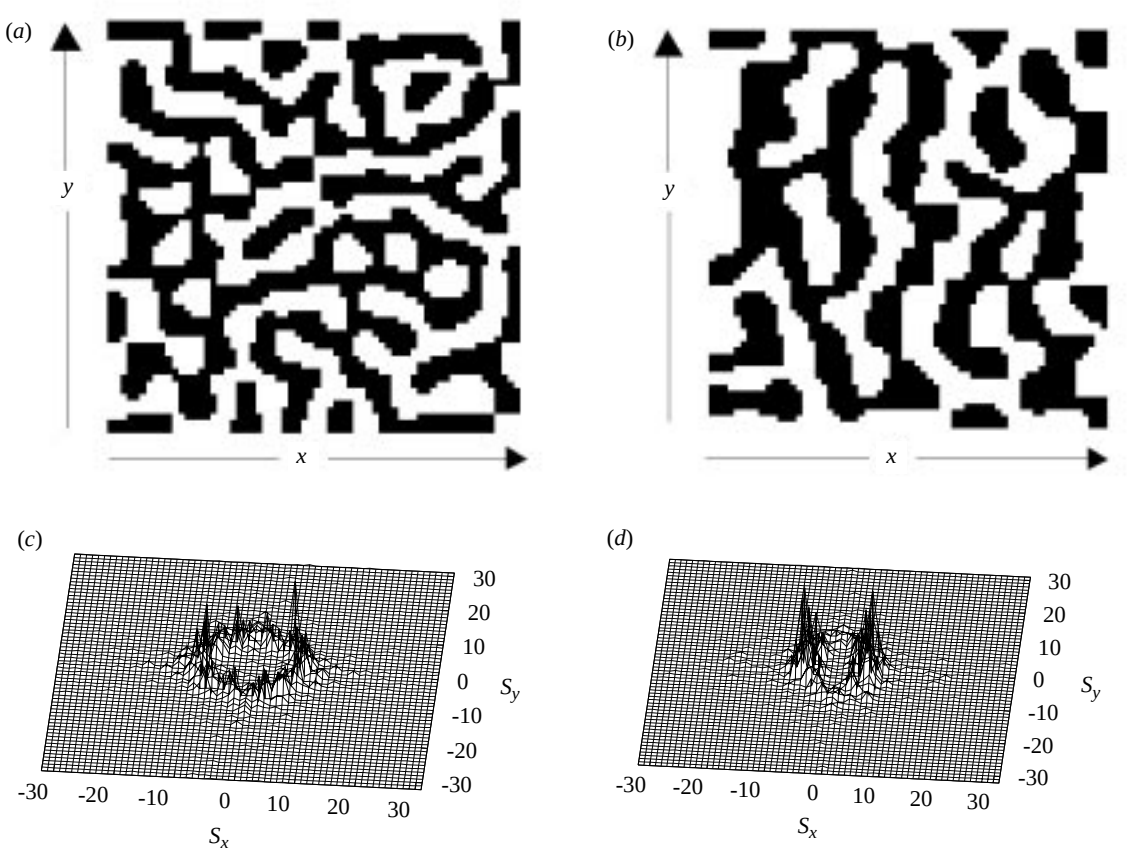

Figure 2. Effect of anisotropic correlations. To simplify the effect at the boundaries, both retinal and cortical units are arranged in square arrays. (*a*) Normal case: 45 by 45 retina (square grid) and 64 by 64 cortex. The black regions are cortical points captured by one retina and white regions are cortical points captured by the other retina. Separation of retinal points: $d_x = d_y = 0.022$. (*c*) Ring-like power spectrum of image in (*a*) consistent with no preferred orientation of the columns (S_x, S_y are spatial frequencies in x and y directions). (*b*) Anisotropic correlations: d_x has been multiplied by 0.6, with d_y left unchanged. The bias towards stripes oriented parallel to the y axis is confirmed by the power spectrum shown in (*d*). Other parameters: $l = 0.08$, $\alpha = 0.2$, $\beta = 4.0$, $k_{\mathrm{init}} = 0.2$, annealing rate is 0.995 (i.e. k was multiplied by 0.995 after each iteration). The initial position of each cortical point was chosen randomly from the volume bounded by the two retinae. Simulations were terminated when the ocular dominance pattern was invariant to further reduction in k.

interaction between the points, and is gradually reduced at a fixed rate at each iteration of the algorithm. Reducing k reduces the range over which the LGN points compete for regions of the cortical sheet. The energy function describing the effect of these two forces is

$$E = -\alpha k \sum_i \log \sum_j \Phi(|\boldsymbol{x}_i - \boldsymbol{y}_j|, k) + \tfrac{1}{2}\beta \sum_j |\boldsymbol{y}_{j+1} - \boldsymbol{y}_j|^2, \qquad (4)$$

where E has the property that $\Delta \boldsymbol{y}_j = -k(\partial E/\partial \boldsymbol{y}_j)$ (Durbin & Willshaw 1987; Durbin *et al.* 1989). It has been shown that certain types of models based on local learning rules are related to the elastic net representation. Both are instantiations, under different assumptions, of the same more abstract objective function (Simic 1990; Yuille 1990; Dayan 1993; Yuille *et al.* 1991, 1996). For the simulations reported in this paper a more efficient optimization proceedure than steepest descent was used (Durbin & Mitchison 1990).

Previous work with this representation of the mapping problem suggested that ocular dominance column spacing would be wider in the cortex of strabismic cats (Goodhill & Willshaw 1990). Recent experimental work confirms this (Löwel 1994), suggesting that more global features of map formation may also be explained by an influence of input correlations (Goodhill & Löwel 1995). In this paper, we investigate the effect of two types of changes to the previously studied uniform correlational structure of the input. First, we introduce a foveal region of increased density of retinal points, representing stronger correlations between neighbouring retinal ganglion cells in the fovea. Second, we introduce anisotropic correlations by 'squashing' the two retinal sheets so that the spacing between points is less in one direction than the other. A possible source for such anisotropic correlations is described in § 5.

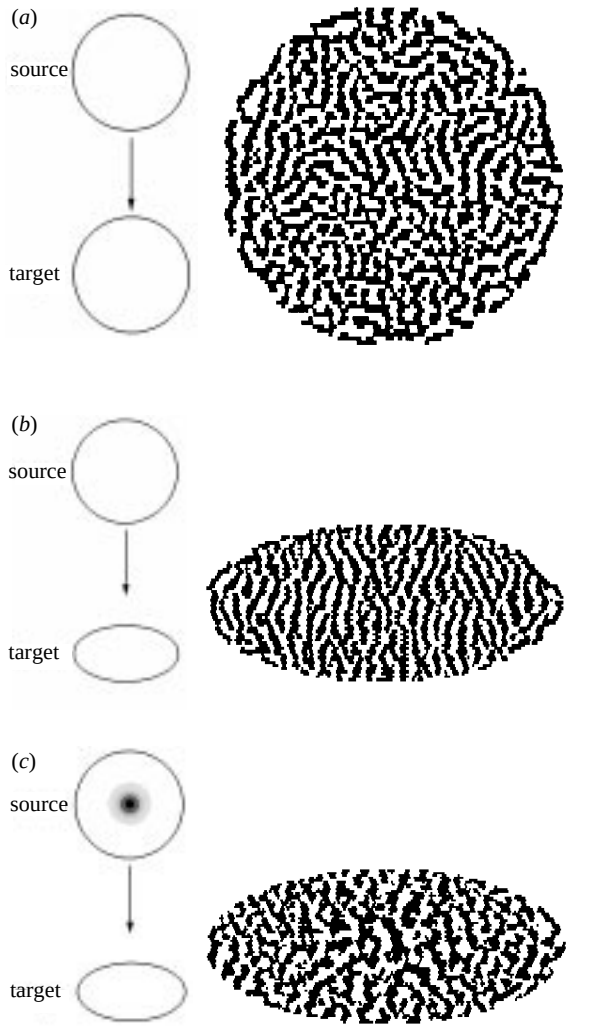

Figure 3. In (*a*) and (*b*) there are 2376 retinal units isotropically arranged in two hexagonal arrays, with roughly the same number of cortical units as retinal units in each picture. In (*a*) these are arranged in a disc of constant radius, while in (*b*) they are arranged in an ellipse of aspect ratio 2:1 (indicated in cartoon form on the left). The bias in the latter picture towards stripes oriented parallel to the short axis of the ellipse can be clearly seen. Other parameters: $l = 0.1$, $\alpha = 0.2$, $\beta = 2.0$, $k_{\text{init}} = 0.2$, annealing rate = 0.98 (see Bauer (1995) for a discussion of the parameter regime where this effect occurs). (*c*) Here an elliptical foveal region of higher source point density was added in the middle of the source arrays (cartoon on left). An increase in disorder and a thickening of the stripes can be seen in this region. The latter follows from the expression for the optimal stripe width in equation 6: d is reduced in the fovea. Parameters: total number of retinal units is 8574, total number of cortical units = 8598, $l = 0.05$, $\alpha = 0.2$, $\beta = 2.0$, $k_{\text{init}} = 0.2$, annealing rate is 0.985.

3. RESULTS

Figure 2 shows the individual contribution of anisotropic correlations to the periodicity and overall alignment of ocular dominance columns. Figure 2*a* shows the ocular dominance map that forms when two retinae of size 45×45 points are mapped onto a single cortical sheet of size 64 by 64 points under the influence of isotropic correlations within each retina, i.e. retinal points are spaced evenly on a square array (other parameter values are given in the figure legends). The black zones are cortical points captured by one retina and the white zones are cortical points captured by the other retina. The columns have no overall preferred orientation; an impression confirmed by the ring-like fourier power spectrum of the image (figure 2*c*). The influence of anisotropic input correlations on the same mapping is shown in figure 2*b*. In this case, the retinal arrays have been squashed along one dimension, equivalent to introducing input correlations that are stronger along one dimension than the orthogonal dimension. The columns now tend to line up *perpendicular* to the direction of stronger correlations, a result that can be explained theoretically by examining directly the energy of two extreme cases for stripe alignment (see next section). The alignment and thickening of the columns suggested by the picture is confirmed by the power spectrum shown in figure 2*d*.

Figure 3 illustrates the influence of target shape and a foveal region on the overall ocular dominance mapping that forms. In figure 3*a*, two circular retinae form a mapping with a circular cortical sheet. The number of retinal units and cortical units are matched, and correlations in the source space are isotropic as in figure 3*a*. No overall orientation to the ocular dominance columns develops. In figure 3*b*, the retinal arrays are still circular and correlations isotropic, but the shape of the cortical sheet has changed to ellipsoidal: there are now more points along one axis than the other (ratio 2:1). This causes the columns to line up parallel to the short axis of the cortical sheet. In figure 3*c*, conditions are similar to figure 3*b* except for the addition of a foveal region with stronger correlations (smaller spacing between retinal points). The introduction of such a region causes more disordered columns and also a thickening of columns in the foveal representation.

Figure 4 shows all the constraints explored above acting in concert: anisotropic input correlations, shape of target cortical region, and a foveal region in the retinae. The scale of the simulation is matched roughly to the number of columns seen experimentally in the macaque. The model accounts for a number of details of the overall mapping of ocular dominance columns in primary visual cortex: the thickening of the columns in the foveal representation (Horton & Hocking 1996), the increased degree of disorder of the columns in the foveal representation (LeVay *et al.* 1985; Horton & Hocking 1996) and the tendency of the columns to orient orthogonal to the borders of the neighbouring visual area and to align somewhat parallel to the dorsal–ventral axis of the cortex. The increased disorder in the foveal representation results from two competing effects: (1) elliptical shape of the target cortex which causes column alignment parallel to the short axis of the ellipse; and (2) anisotropic input correlations which encourages column alignment in the orthogonal direction. The thickening of the columns in the foveal region results from stronger correlations (decreased spacing of retinal points).

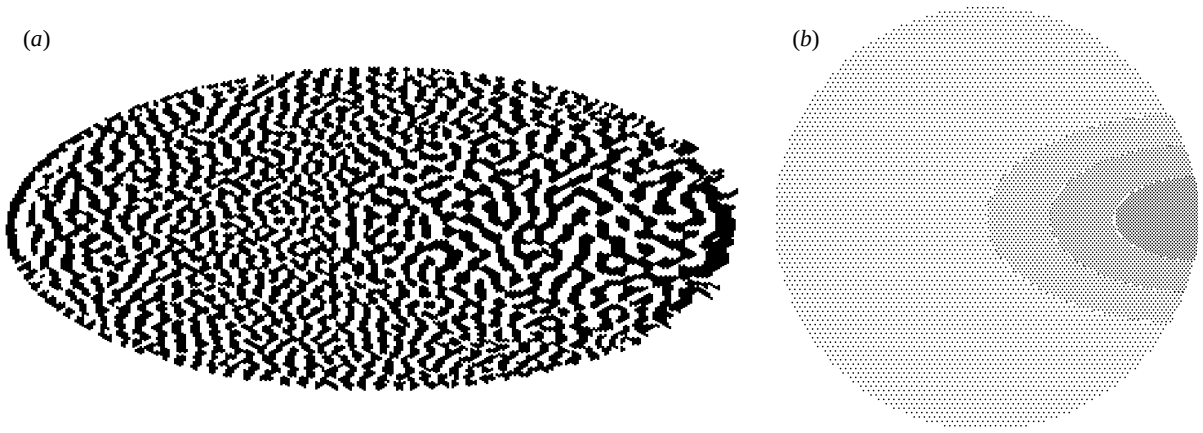

Figure 4. (*a*) Combined effect of globally anisotropic correlations, a foveal region, and elliptical target shape, on the overall stripe pattern. Parameters: total number of retinal units is 16 674, total number of cortical units is 30 393, aspect ratio of cortical ellipse is 2.3:1, $l = 0.02$, $\alpha = 0.2$, $\beta = 2.0$, annealing rate is 0.98. In order to ensure correct overall orientation of the cortex $k_{\text{init}} = 0.05$, and cortical points were initially topographically ordered with a small random ocular bias. (*b*) The distribution of retinal units used to produce the picture shown in (*a*) (same orientation). The separation between retinal units perpendicular to the vertical midline was 0.012 in the 'periphery', 0.010 in the 'macula', 0.009 in the 'perifovea' and 0.008 in the 'fovea'. Parallel to the vertical midline, these distances were multiplied by factors of 1.0 in the periphery, 0.8 in the macula, 0.7 in the perifovea and 0.6 in the fovea. Note that these separations represent correlational relationships rather than physical distances. The circular shape of the boundary of the region represents our lack of knowledge of the detailed variation in correlations at the boundary in different parts of the retina: all parts are treated equally.

4. ANALYSIS OF COLUMN ORIENTATION WITH ANISOTROPIC CORRELATIONS

The explicit objective function for the elastic net allows the direct calculation of the cost of certain solutions for simple arrangements of points. Here we perform a simple analysis of column orientation in the case where there are anisotropic correlations. The analysis proceeds in the following stages. We first calculate the length of a one-dimensional path for columns of fixed width, and optimize this with respect to the column width. Moving then to two dimensions, we consider the case where the within-eye spacing between points in one direction is different from that in the orthogonal direction. The total cost for columns running parallel to each direction is compared.

Consider first the one-dimensional situation shown in figure 5*a*. Refer to the within-eye spacing between points as d and the between-eye spacing as l. For N cells in each eye, the total sum-squared length of the path for columns of width n can be straightforwardly calculated to be L (this is for n even: the formula is slightly different for n odd, but leads to identical conclusions):

$$L = 2N(\tfrac{1}{4}nd^2 + (l^2/n)). \tag{5}$$

Minimizing with respect to n, we find that the minimal length for a columnar solution is when

$$n = 2l/d, \tag{6}$$

as previously described (Goodhill & Willshaw 1990; Goodhill 1992). Substituting this value into equation (5) yields

$$L = 2Nld. \tag{7}$$

Consider now two $N \times N$ arrays on top of each other (see figure 5*b*) with gap l and within-sheet separations d in one direction and $s \times d$ in the other direction, where $s < 1$ is a 'squashing' factor, which determines the degree of anisotropy. For simplicity we compare only two possible arrangements: columns running parallel to the normal direction and columns running parallel to the squashed direction. Which has lower cost? We have N lengths as given in equation (7) plus $2 \times N \times N$ lengths running in the other direction, which join up the paths above. For columns running parallel to the squashed direction this gives a total length of

$$L = 2N^2d[l + s^2d],$$

and for columns running parallel to the normal we have

$$L = 2N^2d[ls + d].$$

Comparing these two lengths yields a condition for columns running parallel to the squashed direction to be favoured:

$$s > (l/d) - 1.$$

Thus, for $(l/d) \geqslant 2$, columns running parallel to the normal direction are always favoured. This may seem counterintuitive, as it says that columns run across rather than along the direction of strongest correlation. However, the simulations shown in figure 2 confirm the analysis.

5. DISCUSSION

We have shown that anisotropic correlations in the input space can significantly influence the overall organization of cortical maps. What could be the

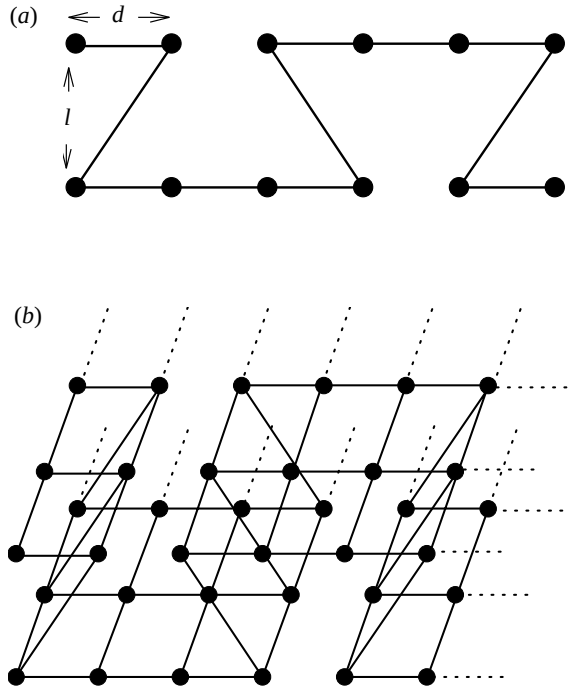

Figure 5. (*a*) A one-dimensional version of the abstract representation used. The dots represent retinal cells, and the distances between them represent correlations. There are two rows, one representing the left eye and one representing the right eye. Cells are regularly spaced with separation d within an eye, and the two eyes are separated by a gap l. As l increases, the correlation between the two eyes decreases. The line represents the topology of the mapping to the cortex. The particular mapping shown is that of regular columns of width $n = 4$ cells. It can be shown that the optimal column width in this representation is $n = (2l/d)$. (*b*) A two-dimensional version of the representation. There are two sheets of dots representing retinal cells, each in a square array, separated by a small gap. The particular mapping to the cortex shown is that of parallel columns of width 4 cells.

biological origin of such correlational anisotropy in the retina? In the area centralis of cat and monkey retina, isodensity contours for retinal ganglion cells (RGCs) form roughly concentric ellipsoidal shapes (Rapaport & Stone 1984; Perry & Cowey 1985) and there is a decrease in RGC density proceeding from central to peripheral retina (Wassle *et al.* 1990). In the cat, the progression to this mature state takes place rapidly where both maturation of synaptic circuitry and RGC density expand as ellipsoidal regions centered on the area centralis (Rapaport & Stone 1984). Although data for primates are more sparse, there is some evidence that a similar process may be occurring (LaVail *et al.* 1991; Provis *et al.* 1985; Van Driel *et al.* 1990) and that a central to peripheral gradient of development also exists for RGC afferents terminating in the lateral geniculate nucleus (Lachica & Casagrande 1988). The degree of anisotropy in the development of local connections between RGCs is not known. It is possible that, as a result of spontaneous activity before visual experience (Galli & Meaffei 1988; Meister *et al.* 1991; Wong *et al.* 1995) the ellipsoidal contours for RGC development impose anisotropic spatial structure on the correlations in early RGC spike production, and that this anisotropy in correlational structure is passed on to the primary visual cortex.

While the basic pattern of ocular dominance segregation in the monkey appears to be complete before birth (Horton & Hocking 1996) in the cat segregation occurs after eye opening. The correlational structure of natural scenes is slightly anisotropic (Hancock *et al.* 1992; van der Schaaf & van der Hateren 1996), though presumably not enough to influence the usually disorded ocular dominance column pattern. However, the model predicts that raising kittens in a strongly anisotropic visual environment (for instance with cylindrical lenses) should introduce some global order into the pattern. In particular, the model predicts that columns will tend to line up parallel to the direction of *weaker* correlations.

Although the elastic net embodies a number of features common to many developmental models, its previous incarnations have not accounted for global aspects of map structure. The success of the current model strengthens previous suggestions that, although many biological mechanisms are at work in the cortex, they may collectively act to satisfy two broad categories of constraints: matching and smoothing. The results further suggest that factors that influence the interaction of input correlations and target shape can exert control over global features of map organization, thus controlling the way that a given region of cortex organizes and represents information. Hence, factors that define the ontogeny of the shapes of competent regions in source and target will exert a powerful influence on global map structure. In any area of the cortex, it is easy to imagine that various neurotrophic and/or neurotropic factors could define different shaped target regions for different classes of axons invading the common area. Our assumption about anisotropic correlational structure in the retina is also a version of this viewpoint: some set of intrinsic retinal mechanisms structures the development of competent regions of retina and induces larger scale spatial structure in the activity patterns that are sent along to more central targets. It is possible that a closer theoretical examination of these kinds of interactions can yield insights into map formation throughout the cortex.

This work was supported by National Institute of Mental Health and the Center for Theoretical Neuroscience at Baylor College of Medicine (P.R.M.). We are grateful to Peter Dayan, Jonathon Horton and David Rapaport for helpful criticisms, and Christophe Person for help with computer simulations.

REFERENCES

Bauer, H.-U. 1995 Development of oriented ocular dominance bands as a consequence of areal geometry. *Neural Comp.* **7**, 36–50.

Berns, G. S., Dayan, P. S. & Sejnowski, T. J. 1993 A correlational model for the development of disparity selectivity in visual cortex that depends on prenatal

and postnatal phases. *Proc. Natn. Acad. Sci. USA* **90**, 8277–8281.

Dayan, P. S. 1993 Arbitrary elastic topologies and ocular dominance. *Neural Comp.* **5**, 392–401.

Durbin, R. & Mitchison, G. 1990 A dimension reduction framework for understanding cortical maps. *Nature* **343**, 644–647.

Durbin, R., Szeliski, R. & Yuille, A. 1989 An analysis of the elastic net approach to the traveling salesman problem. *Neural Comp.* **1**, 348–358.

Durbin, R. & Willshaw, D. J. 1987 An analogue approach to the travelling salesman problem using an elastic net method. *Nature* **326**, 689–691.

Erwin, E., Obermayer, K. & Schulten, K. 1995 Models of orientation and ocular dominance columns in the visual cortex: a critical comparison. *Neural Comp.* **7**, 425–468.

Galli, L. & Maffei, L. 1988 Spontaneous impulse activity of rat retinal ganglion cells in prenatal life. *Science* **242**, 90–91.

Goodhill, G. J. 1992 Correlations, competition and optimality: modelling the development of topography and ocular dominance. Cognitive Science Research Paper CSRP 226, University of Sussex.

Goodhill, G. J. & Löwel, S. 1995 Theory meets experiment: correlated neural activity helps determine ocular dominance column periodicity. *Trends Neurosci.* **18**, 437–439.

Goodhill, G. J. & Willshaw, D. J. 1990 Application of the elastic net algorithm to the formation of ocular dominance stripes. *Network* **1**, 41–59.

Goodhill, G. J. & Willshaw, D. J. 1994 Elastic net model of ocular dominance: overall stripe pattern and monocular deprivation. *Neural Comp.* **6**, 615–621.

Hancock, P. J. B., Baddeley, R. J. & Smith, L. S. 1992 The principal components of natural images. *Network* **3**, 61–70.

Horton, J. C. & Hocking, D. R. 1996 An adult-like pattern of ocular dominance columns in striate cortex of newborn monkeys prior to visual experience. *J. Neurosci.* **16**, 1791–1807.

Hubel, D. H. & Wiesel, T. N. 1977 Functional architecture of the macaque monkey visual cortex. *Proc. R. Soc. Lond.* B **198**, 1–59.

Jones, D. G., Van Sluyters, R. C. & Murphy, K. M. 1991 A computational model for the overall pattern of ocular dominance. *J. Neurosci.* **11**, 3794–3808.

Lachica, E. A. & Casagrande, V. A. 1988 Development of primate retinogeniculate axon arbors. *Vis. Neurosci.* **1**, 103–123.

LaVail, M. M., Rapaport, D. H. & Rakic, P. 1991 Cytogenesis in the monkey retina. *J. Comp. Neurol.* **309**, 86–114.

LeVay, S., Connolly, M., Houde, J. & Van Essen, D. C. 1985 The complete pattern of ocular dominance stripes in the striate cortex and visual field of the macaque monkey. *J. Neurosci.* **5**, 486–501.

Löwel, S. 1994 Ocular dominance column development: strabismus changes the spacing of adjacent columns in cat visual cortex. *J. Neurosci.* **14**, 7451–7468.

Malsburg, C. von der 1973 Self-organization of orientation sensitive cells in the striate cortex. *Kybernetik* **14**, 85–100.

Malsburg, C. von der & Willshaw, D. J. 1976 A mechanism for producing continuous neural mappings: ocularity dominance stripes and ordered retino-tectal projections. *Expl Brain. Res.* suppl. 1, 463–469.

Meister, M., Wong, R. O. L., Baylor, D. A. & Shatz, C. J. 1991 Synchronous bursts of action potentials in ganglion cells of the developing mammalian retina. *Science* **252**, 939–943.

Obermayer, K., Ritter, H. & Schulten, K. 1990 A principle for the formation of the spatial structure of cortical feature maps. *Proc. Natn. Acad. Sci. USA* **87**, 8345–8349.

Obermayer, K., Blasdel, G. G. & Schulten, K. 1992 Statistical-mechanical analysis of self-organization and pattern formation during the development of visual maps. *Phys. Rev.* A **45**, 7568–7589.

Perry, V. H. & Cowey, A. 1985 The ganglion cell and cone distributions in the monkey's retina: implications for central magnification factor. *Vis. Res.* **25**, 1795–1810.

Provis, J. M., Van Driel, D., Billson, F. A. & Russell, P. 1985 Development of the human retina—patterns of cell distribution and redistribution in the ganglion-cell layer. *J. Comp. Neurol.* **233**, 429–451.

Rapaport, D. H. & Stone, J. 1984 The area centralis of the retina in the cat and other mammals: focal point for function and development of the visual system. *Neuroscience* **11**, 289–301.

Schaaf, A. van der & Hateren, J. H. van der 1996 Modeling the power spectra of natural images—statistics and information. *Vis. Res.* **36**, 2759–2770.

Simic, P. D. 1990 Statistical mechanics as the underlying theory of 'elastic' and 'neural' optimisations. *Network* **1**, 89–103.

Swindale, N. V. 1980 A model for the formation of ocular dominance stripes. *Proc. R. Soc. Lond.* B **208**, 243–264.

Swindale, N. V. 1996 The development of topography in the visual cortex: a review of models. *Network* **7**, 161–247.

Van Driel, D., Provis, J. M. & Billson, F. A. 1990 Early differentiation of ganglion, amacrine, bipolar, and Muller cells in the developing fovea of human retina. *J. Comp. Neurol.* **291**, 203–219.

Wassle, H., Grunert, U., Rohrenbeck, J. & Boycott, B. B. 1990 Retinal ganglion-cell density and cortical magnification factor in the primate. *Vis. Res.* **30**, 1897–1911.

Wolf, F., Bauer, H.-U. & Geisel, T. 1994 Formation of field discontinuities and islands in visual cortical maps. *Biol. Cyber.* **70**, 525–531.

Wolf, F., Bauer, H.-U., Pawelzik, K. & Geisel, T. 1996 Organization of the visual cortex. *Nature* **382**, 306.

Wong, R. O. L., Chernjavsky, A., Smith, S. J. & Shatz, C. J. 1995 Early functional neural networks in the developing retina. *Nature* **374**, 716–718.

Yuille, A. L. 1990 Generalized deformable models, statistical physics, and matching problems. *Neural Comp.* **2**, 1–24.

Yuille, A. L., Kolodny, J. A. & Lee, C. W. 1991 Dimension reduction, generalized deformable models and the development of ocularity and orientation. *Int. Joint Conf. on Neural Networks, Seattle, July 1991*, vol. II, pp. 597–602.

Yuille, A. L., Kolodny, J. A. & Lee, C. W. 1996 Dimension reduction, generalized deformable models and the development of ocularity and orientation. *Neural Networks* **9**, 309–319.

Received 14 November 1996; accepted 26 November 1996